ENGINEERING RESEARCH INSTITUTE
THE UNIVERSITY OF MICHIGAN
ANN ARBOR

Progress Report

A METHOD FOR CORRECTING AERIAL PHOTOGRAPHS FOR IMAGE DISPLACEMENT CAUSED BY SUPERSONIC SHOCK WAVES WHEN THE SHOCK-WAVE CHARACTERISTICS ARE KNOWN

W. H. Ball
E. Young
J. M. Vukovich

ERI Project 2426

RAYTHEON MANUFACTURING COMPANY
MAYNARD LABORATORY
MAYNARD, MASSACHUSETTS

May 1958

ABSTRACT

In supersonic flight, the images in an aerial metric camera with optical axis vertical, or nearly so, will have displacements varying in magnitude depending on the angular positions of the ground objects with respect to the optical axis of the camera and the configuration of the shock wave. In this discussion a 120° cone* is assumed as the shock-wave pattern and the angular field of the camera is taken as 90 degrees. The effect of refraction due to boundary layer is mentioned in the text and reference is given to work done on this subject.

*See schlieren photographs in Reference 1.

INTRODUCTION

There are two main effects in supersonic flights that result in refraction of an image ray while taking aerial photographs. One of these is caused by the boundary layer which is the transition zone where a change in wall to free-stream temperature occurs. This temperature differential changes the density of the air across the boundary layer and hence causes the incident image ray to be refracted. Graphical representations of this deviation plotting $\delta/\tan\theta_i$ vs. T_w/T_∞ for altitudes from 0 to 75,000 feet, where δ is the deviation in seconds of arc, θ_i is the angle of incidence of the light ray, T_w is the wall temperature, and T_∞ is the free-stream temperature, have been presented in a report by M. P. Moyle and R. E. Cullen. These graphs, or graphs similar to them, could easily be used to correct the aerial photogaph for deviations caused by the boundary layer. From the shape of the curves, it would be a simple matter to program an analytic correction procedure.

The other of these effects is caused by the bending of an image ray when passing through the shock wave. In this discussion it has been assumed that information on the shock-wave configuration, as well as information on how a light ray is bent while passing at various angles of incidence through a shock wave, could be made available to us.

DISCUSSION

From the report by Moyle and Cullen it seemed reasonable to assume that the shock-wave pattern could be represented by a 120° cone. To begin with, the equations for the family of cones representing varying field angles for a vertical camera were computed. We let θ equal one-half the field angle and computed the family of camera or image cones for 5° increments of θ. Next the intersection of the 120° shock-wave cone and the camera cone with $\theta = 45°$ was computed (see Fig. 1). The initial point of intersection of these two cones has coordinates $(0,-0.634d,-0.634d)$, where d is the distance from the apex of the shock-wave cone to the camera (see Fig. 2). Then the family of circles corresponding to the locus of all points where an incident image ray intersects the shock wave at some angle α was computed. This family was computed for 5° increments of α. In Fig. 1 the circles for $\alpha = 75°$ and for $\alpha = 30°$ are displayed. These circles have equations of the form $x^2 + z^2 = r^2$ lying in a plane associated with a particular value of y. For example, the circle corresponding to $\alpha = 75°$ is represented by $x^2 + z^2 = (0.634d)^2 = 0.4020d^2$ lying in the plane $y = -0.634d$. Then the intersection of each of these equal α

circles with each of the family of image cones was computed. The images on the photographic plane of these intersections were now desired. To obtain these it is necessary to project back through the lens, but since these intersections do not lie in a plane, a further correction has to be made (see Figs. 3 and 4). Note that, after this correction, the images of the intersections, written in X,Y coordinates, are functions of f, the focal length of the camera, and are independent of d. Figure 5 is the final plotting of a photographic plate with the images of the intersections for various values of α. These curves are hyberbolic and exhibit symmetry about the X and Y axes. As an example of the method of correction, any point on the line $\alpha = 50°$ would have been deviated by some specified amount, whatever the deviation a light ray passing through a shock wave at a 50° angle of incidence was found to be. Since a vertical camera was assumed, the correction is radial to the principal point. Naturally, interpolation would be necessary for those image points on the photo which did not fall on a line corresponding to a tabulated value of α. Note that the system is not symmetric with respect to the camera angle θ. Hence it is thought that a graphical correction would be simpler to obtain than an analytic correction. An immediate method of correction would be to produce a copy of Fig. 5 the size of a 9-1/2-by-9-1/2-inch photo and to superimpose this copy on a photo to see where the images of the control points fall, and correct accordingly. At any rate, further efforts will be made to obtain an analytic correction method.

It seems advisable to discuss the various assumptions that were made as well as the changes that would occur if the assumptions were not valid.

1. A 120° shock-wave cone was assumed. In applying a correction of this type, it would be necessary to know the actual shock-wave configuration for the plane in use. The shock wave may not be strictly conical, in which case this method would have to be modified or discarded depending on how great the deviation from a conical shape was. The cone may have an apex angle not equal to 120°, but this could easily be corrected for by changing the equation for the shock-wave cone in an appropriate manner. There also may be a series of shock waves of this type, in which case a repeated application of this method could be applied.

2. A vertical camera, that is, zero tilt, was assumed. If there is a departure from verticality, two things occur. First, symmetry about the principal point is destroyed. Second, corrections would be radial to the nadir point for tilted photographs and not to the principal point as when zero tilt is the case. In low-tilt photographs the magnitude of the change this introduces is probably such that it could be ignored.

3. The apex of the shock-wave cone and the camera were assumed to lie on the longitudinal axis of the plane. If the camera were mounted outside the longitudinal axis, symmetry would occur about both the image of the line connecting the camera and the apex of the shock-wave cone, and about a line perpendicular to this line through the principal point of the photo if the camera

were not tilted. With an offset, tilted camera, there would be a combination of these effects.

One other point remains to be mentioned and it is something that would have to be investigated further. For a particular velocity of the plane, there is a particular shock-wave configuration and a particular shock-wave strength. For a different velocity, the shock-wave configuration probably remains relatively the same but the wave strength changes. Thus, the manner in which a light ray is bent while passing at various angles through a shock wave is probably a function of the wave strength and hence of the Mach number.

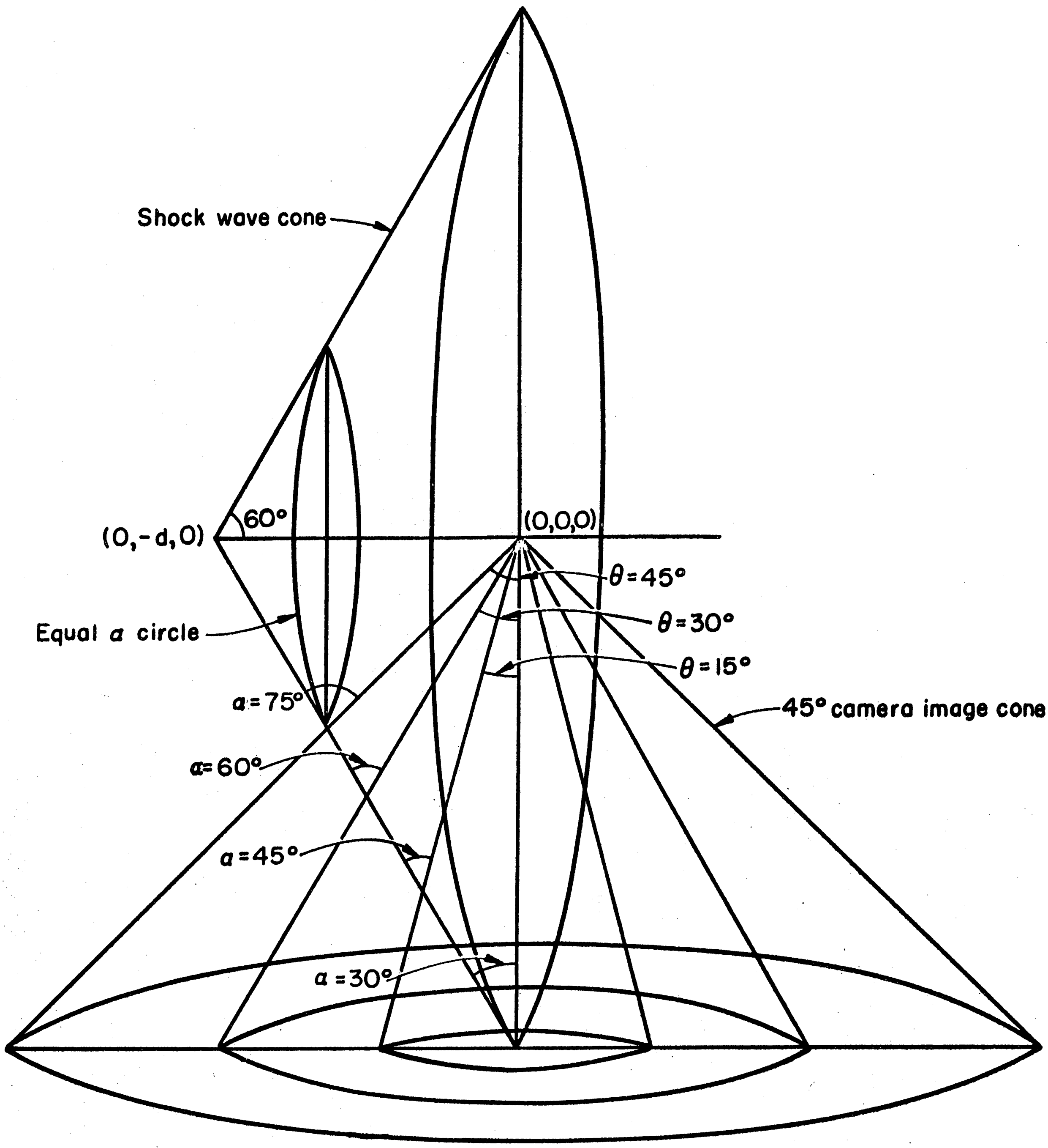

Fig. 1. Intersection of 120° shock-wave cone with family of camera cones.

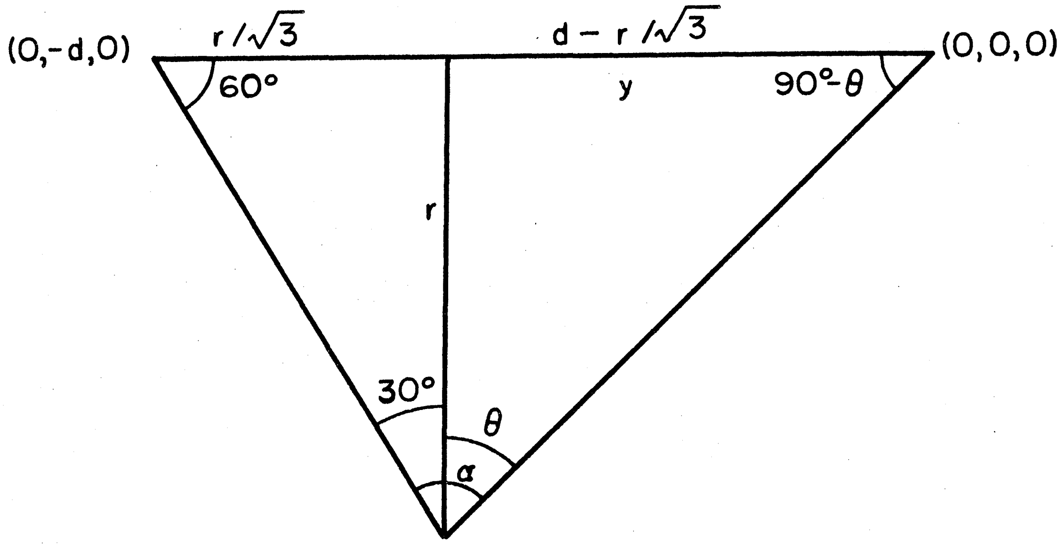

$$\tan \theta = \frac{d - r/\sqrt{3}}{r} \qquad \tan \theta = \frac{y}{r}$$

$$r \tan \theta = d - r/\sqrt{3} \qquad y = r \tan \theta$$

$$r = \frac{d}{\tan \theta + \tan 30°}$$

Fig. 2. Radius of equal α circles.

The family of image cones is given by $(\cot^2 \theta)(x^2 + y^2) - z^2 = 0$

45° cone: $1.0000\ (x^2 + y^2) - z^2 = 0$

40° cone: $1.4204\ (x^2 + y^2) - z^2 = 0$

35° cone: $2.0395\ (x^2 + y^2) - z^2 = 0$

30° cone: $3.0000\ (x^2 + y^2) - z^2 = 0$

25° cone: $4.5989\ (x^2 + y^2) - z^2 = 0$

20° cone: $7.5488\ (x^2 + y^2) - z^2 = 0$

15° cone: $13.9286\ (x^2 + y^2) - z^2 = 0$

10° cone: $32.1636\ (x^2 + y^2) - z^2 = 0$

5° cone: $130.6449\ (x^2 + y^2) - z^2 = 0$

The equations for the equal α circles are as follows:

α	r	y	$x^2 + z^2$
75°	0.634d	-0.634d	$0.4020d^2$
70°	0.706d	-0.592d	$0.4984d^2$
65°	0.783d	-0.548d	$0.6131d^2$
60°	0.866d	-0.500d	$0.7500d^2$
55°	0.958d	-0.447d	$0.9178d^2$
50°	1.062d	-0.387d	$1.1278d^2$
45°	1.183d	-0.317d	$1.3995d^2$
40°	1.327d	-0.234d	$1.7609d^2$
35°	1.504d	-0.132d	$2.2620d^2$
30°	1.732d	0.000d	$3.0000d^2$
25°	2.041d	0.179d	$4.1657d^2$
20°	2.494d	0.440d	$6.2200d^2$
15°	3.232d	0.866d	$10.4458d^2$
10°	4.686d	1.706d	$21.9586d^2$
5°	9.006d	4.200d	$81.1080d^2$

The results of the computation for the initial intersection curves between the equal α circles and the family of image cones are as follows:

α	cone	x	y	z
75°	45°	0.000d	-0.634d	-0.634d
70°	45°	±0.272d	-0.592d	-0.652d
70°	40°	0.000d	-0.592d	-0.706d
65°	45°	±0.395d	-0.548d	-0.676d
65°	40°	±0.278d	-0.548d	-0.732d
65°	35°	0.000d	-0.548d	-0.783d
60°	45°	±0.500d	-0.500d	-0.707d
60°	40°	±0.404d	-0.500d	-0.766d
60°	35°	±0.281d	-0.500d	-0.819d
60°	30°	0.000d	-0.500d	-0.866d
55°	45°	±0.599d	-0.447d	-0.748d
55°	40°	±0.512d	-0.447d	-0.810d
55°	35°	±0.410d	-0.447d	-0.866d
55°	30°	±0.282d	-0.447d	-0.916d
55°	25°	0.000d	-0.447d	-0.958d
50°	45°	±0.699d	-0.387d	-0.799d
50°	40°	±0.615d	-0.387d	-0.866d
50°	35°	±0.520d	-0.387d	-0.926d
50°	30°	±0.411d	-0.387d	-0.979d
50°	25°	±0.280d	-0.387d	-1.024d
50°	20°	0.000d	-0.387d	-1.062d
45°	45°	±0.806d	-0.317d	-0.866d
45°	40°	±0.721d	-0.317d	-0.938d
45°	35°	±0.627d	-0.317d	-1.003d
45°	30°	±0.524d	-0.317d	-1.061d
45°	25°	±0.409d	-0.317d	-1.110d
45°	20°	±0.274d	-0.317d	-1.151d
45°	15°	0.000d	-0.317d	-1.183d

α	cone	x	y	z
40°	45°	±0.924d	-0.234d	-0.953d
40°	40°	±0.834d	-0.234d	-1.032d
40°	35°	±0.737d	-0.234d	-1.104d
40°	30°	±0.632d	-0.234d	-1.167d
40°	25°	±0.519d	-0.234d	-1.221d
40°	20°	±0.397d	-0.234d	-1.266d
40°	15°	±0.266d	-0.234d	-1.300d
40°	10°	0.000d	-0.234d	-1.327d
35°	45°	±1.059d	-0.132d	-1.068d
35°	40°	±0.961d	-0.132d	-1.157d
35°	35°	±0.856d	-0.132d	-1.237d
35°	30°	±0.743d	-0.132d	-1.308d
35°	25°	±0.624d	-0.132d	-1.368d
35°	20°	±0.499d	-0.132d	-1.419d
35°	15°	±0.352d	-0.132d	-1.462d
35°	10°	±0.226d	-0.132d	-1.487d
35°	5°	0.000d	-0.132d	-1.504d
30°	45°	±1.225d	0.000d	-1.225d
30°	40°	±1.113d	0.000d	-1.327d
30°	35°	±0.993d	0.000d	-1.419d
30°	30°	±0.866d	0.000d	-1.500d
30°	25°	±0.732d	0.000d	-1.570d
30°	20°	±0.592d	0.000d	-1.628d
30°	15°	±0.448d	0.000d	-1.673d
30°	10°	±0.301d	0.000d	-1.706d
30°	5°	±0.151d	0.000d	-1.725d
30°	0°	0.000d	0.000d	-1.732d
25°	45°	±1.438d	0.179d	-1.449d
25°	40°	±1.305d	0.179d	-1.570d
25°	35°	±1.161d	0.179d	-1.678d
25°	30°	±1.009d	0.179d	-1.774d
25°	25°	±0.847d	0.179d	-1.857d
25°	20°	±0.677d	0.179d	-1.925d
25°	15°	±0.499d	0.179d	-1.979d
25°	10°	±0.307d	0.179d	-2.018d
25°	5°	0.000d	0.179d	-2.041d

α	cone	x	y	z
20°	45°	±1.736d	0.440d	-1.791d
20°	40°	±1.567d	0.440d	-1.940d
20°	35°	±1.384d	0.440d	-2.074d
20°	30°	±1.187d	0.440d	-2.193d
20°	25°	±0.976d	0.440d	-2.295d
20°	20°	±0.746d	0.440d	-2.380d
20°	15°	±0.486d	0.440d	-2.446d
20°	10°	0.000d	0.440d	-2.494d
15°	45°	±2.202d	0.866d	-2.366d
15°	40°	±1.969d	0.886d	-2.563d
15°	35°	±1.713d	0.866d	-2.741d
15°	30°	±1.431d	0.866d	-2.898d
15°	25°	±1.118d	0.866d	-3.033d
15°	20°	±0.749d	0.866d	-3.144d
15°	15°	0.000d	0.866d	-3.232d
10°	45°	±3.086d	1.706d	-3.526d
10°	40°	±2.714d	1.706d	-3.820d
10°	35°	±2.296d	1.706d	-4.085d
10°	30°	±1.818d	1.706d	-4.319d
10°	25°	±1.237d	1.706d	-4.520d
10°	20°	0.000d	1.706d	-4.686d
5°	45°	±5.633d	4.200d	-7.027d
5°	40°	±4.812d	4.200d	-7.612d
5°	35°	±3.853d	4.200d	-8.140d
5°	30°	±2.655d	4.200d	-8.606d
5°	25°	0.000d	4.200d	-9.006d

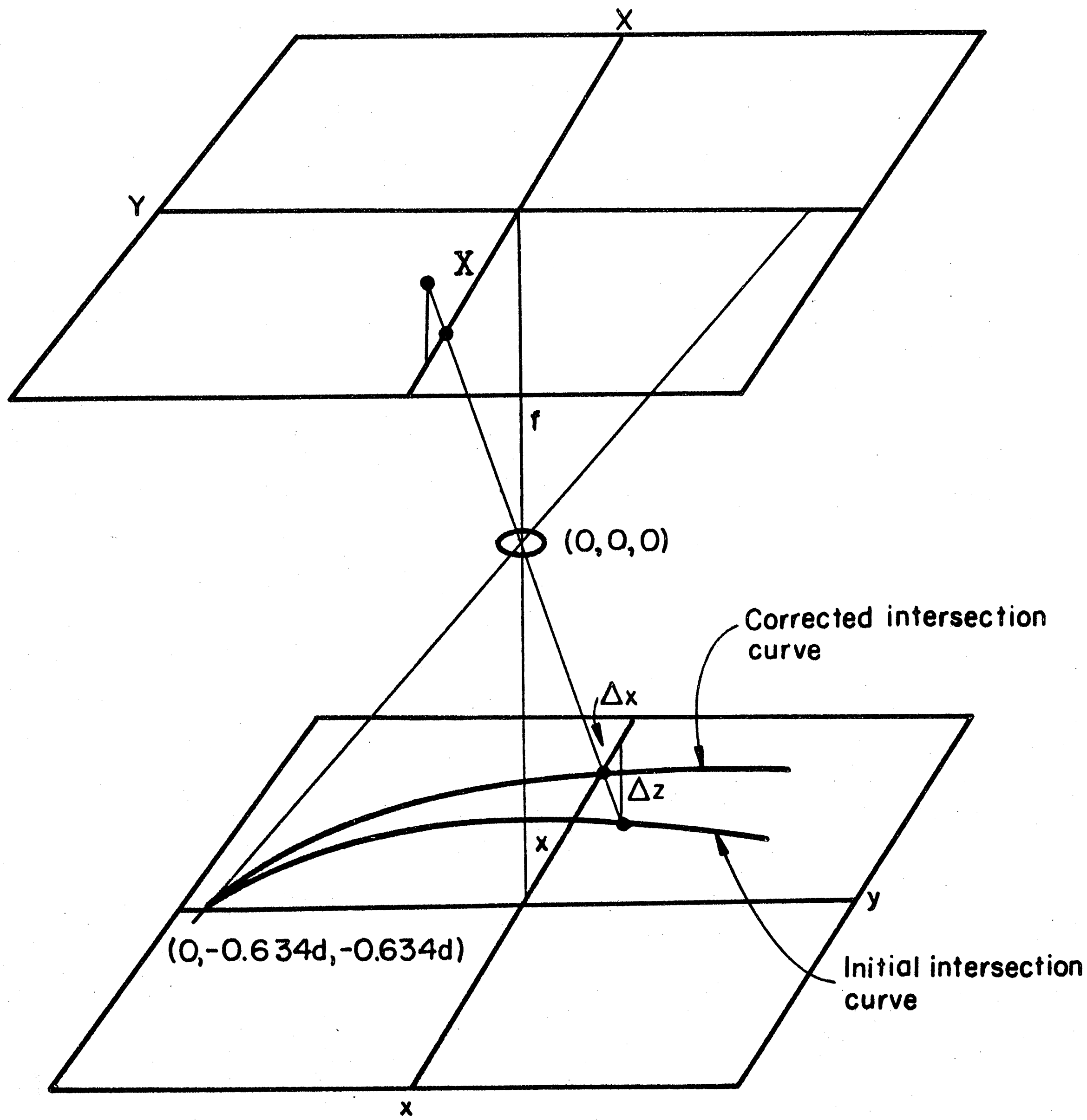

Fig. 3. Projection through camera lens of intersection curves into focal plane.

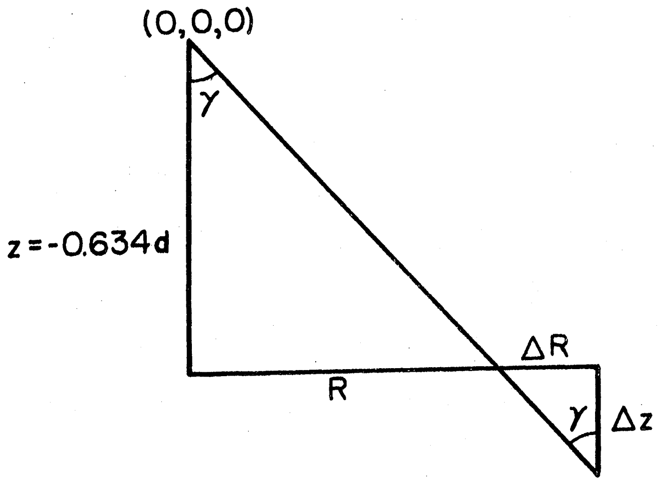

$$R = (x^2 + y^2)^{1/2} \qquad \tan\gamma = \frac{R}{z} = \frac{\Delta R}{\Delta z}$$

$$\Delta R = \Delta z \tan\gamma$$

$$\Delta x = \frac{x}{R}\Delta R \qquad x' = x - \Delta x \qquad X = \frac{f}{0.634d}x'$$

$$\Delta y = \frac{y}{R}\Delta R \qquad y' = y - \Delta y \qquad Y = \frac{f}{0.634d}y'$$

Fig. 4. Z-difference correction to points of intersection.

The results of the computation for the corrected intersection curves are as follows:

α	X	Y
75°	0.000f	-1.00f
70°	±0.416f	-0.909f
70°	0.000f	-0.839f
65°	±0.584f	-0.811f
65°	±0.380f	-0.749f
65°	0.000f	-0.700f
60°	±0.707f	-0.707f
60°	±0.527f	-0.653f
60°	±0.342f	-0.610f
60°	0.000f	-0.577f
55°	±0.801f	-0.598f
55°	±0.632f	-0.552f
55°	±0.473f	-0.516f
55°	±0.308f	-0.487f
55°	0.000f	-0.467f
50°	±0.875f	-0.484f
50°	±0.710f	-0.446f
50°	±0.562f	-0.418f
50°	±0.420f	-0.396f
50°	±0.273f	-0.379f
50°	0.000f	-0.364f
45°	±0.931f	-0.366f
45°	±0.770f	-0.338f
45°	±0.625f	-0.315f
45°	±0.494f	-0.300f
45°	±0.369f	-0.285f
45°	±0.238f	-0.276f
45°	0.000f	-0.268f

α	X	Y
40°	±0.970f	-0.246f
40°	±0.808f	-0.227f
40°	±0.667f	-0.211f
40°	±0.541f	-0.200f
40°	±0.424f	-0.191f
40°	±0.314f	-0.185f
40°	±0.205f	-0.180f
40°	0.000f	-0.177f
35°	±0.992f	-0.123f
35°	±0.831f	-0.114f
35°	±0.692f	-0.107f
35°	±0.568f	-0.101f
35°	±0.456f	-0.096f
35°	±0.352f	-0.093f
35°	±0.241f	-0.090f
35°	±0.153f	-0.088f
35°	0.000f	-0.088f
30°	±1.000f	0.000f

The rest of the α = 30° all lie on the x axis.

α	X	Y
25°	±0.992f	0.125f
25°	±0.831f	0.114f
25°	±0.692f	0.107f
25°	±0.568f	0.101f
25°	±0.456f	0.096f
25°	±0.352f	0.093f
25°	±0.252f	0.090f
25°	±0.153f	0.088f
25°	0.000f	0.088f
20°	±0.970f	0.246f
20°	±0.808f	0.227f
20°	±0.667f	0.213f
20°	±0.541f	0.200f
20°	±0.426f	0.192f
20°	±0.314f	0.185f
20°	±0.199f	0.180f
20°	0.000f	0.177f

α	X	Y
15°	±0.931f	0.364f
15°	±0.768f	0.338f
15°	±0.625f	0.315f
15°	±0.494f	0.298f
15°	±0.369f	0.285f
15°	±0.238f	0.276f
15°	0.000f	0.268f
10°	±0.875f	0.484f
10°	±0.710f	0.446f
10°	±0.562f	0.418f
10°	±0.421f	0.394f
10°	±0.273f	0.377f
10°	0.000f	0.364f
5°	±0.801f	0.596f
5°	±0.632f	0.552f
5°	±0.473f	0.516f
5°	±0.309f	0.489f
5°	0.000f	0.465f

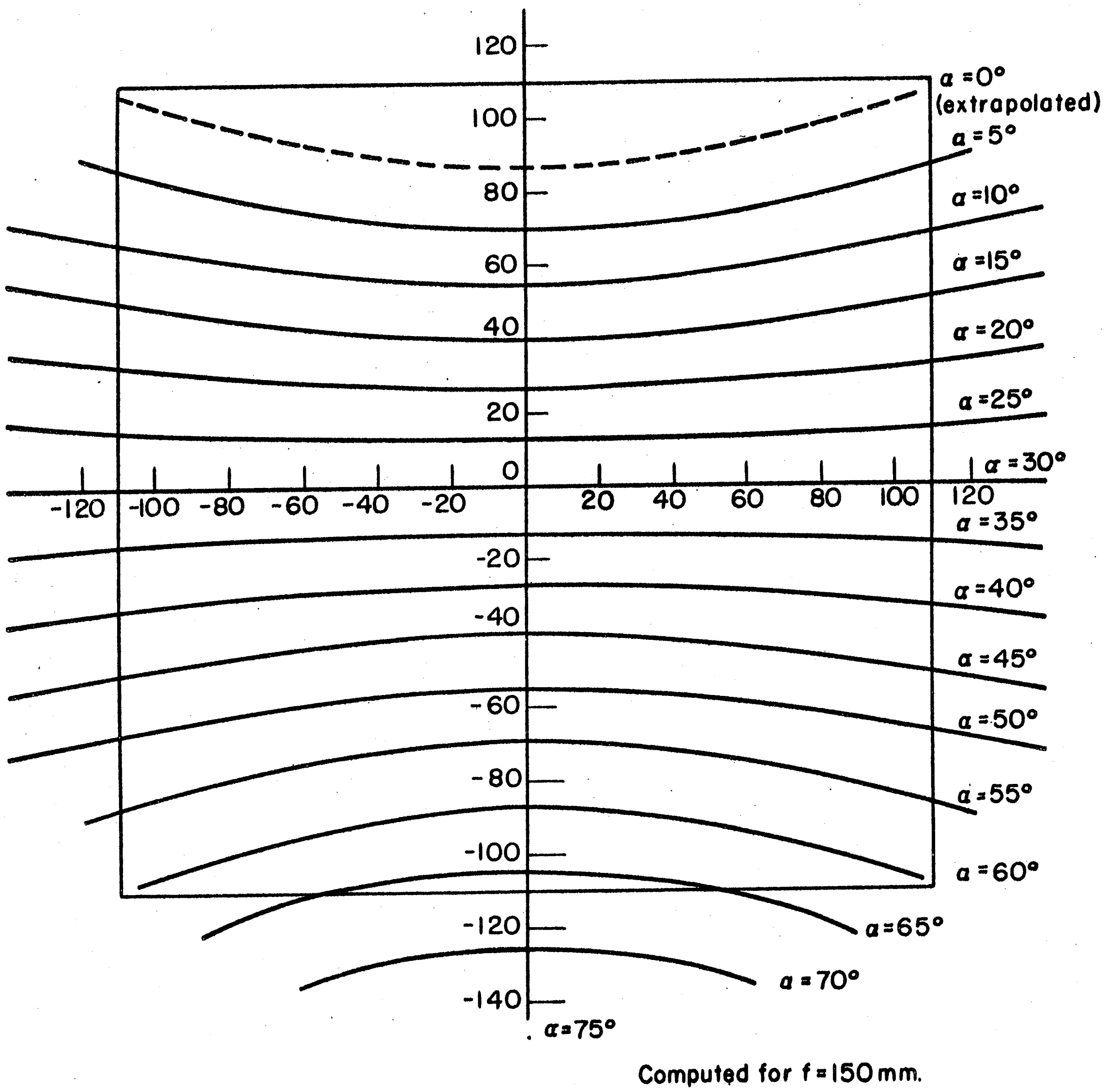

Fig. 5. Plot of equal α curves of intersection.

REFERENCE

1. Moyle, M. P., and Cullen, R. E., Anti-Icing and Anti-Frosting of Aerial Photographic Windows, Univ. of Mich. Eng. Res. Inst. Report 2197-25-F, Ann Arbor, October, 1955.

BIBLIOGRAPHY

1. Moyle, M. P., and Cullen, R. E., Refraction Errors in Aerial Photography at High Flight Speeds, Univ. of Mich. Eng. Res. Inst. Report 2197-14-P, Ann Arbor, May, 1955.

2. Moyle, M. P., and Cullen, R. E., Refraction Errors in Aerial Photography at High Flight Speeds, Univ. of Mich. Eng. Res. Inst. Report 2197-20-P, Ann Arbor, May, 1955.

3. Moyle, M. P., Jackson, P. L., Dabora, E. K., Sherman, P., and Cullen, R.E., Experimental Evaluation of the RF-101 Forward Oblique Window Under Stress and Effect of Air Density Changes on Aerial Photography, Univ. of Mich Eng. Res. Inst. Report 2508-1-F, Ann Arbor, April, 1957.